VOL. 53 NO. 7, JULY 2000 THE JOURNAL OF ANTIBIOTICS pp. 677 — 686

# Kodaistatins, Novel Inhibitors of Glucose-6-phosphate Translocase T1 from *Aspergillus terreus* Thom DSM 11247

## Isolation and Structural Elucidation

LÁSZLÓ VÉRTESY[†,*], HANS-JÖRG BURGER[†], JAYVANTI KENJA[††], MARTIN KNAUF[†], HERBERT KOGLER[†], ERICH F. PAULUS[†], NIROGI V. S. RAMAKRISHNA[††], KESHAVAPURA H. S. SWAMY[††], ERRA K. S. VIJAYAKUMAR[††] and PETER HAMMANN[†]

[†] Hoechst Marion Roussel Deutschland GmbH,
Drug Innovation & Approval, * Natural Product Research, H-780
D-65926 Frankfurt/M, Germany
[††] Hoechst India Limited,
Mumbai-400 080, India

(Received for publication March 3, 2000)

Two novel compounds, kodaistatin A, $C_{35}H_{34}O_{11}$, molecular weight 630, and kodaistatin C, $C_{35}H_{34}O_{12}$, molecular weight 646, have been isolated from cultures of *Aspergillus terreus* Thom DSM 11247 by solid-phase extraction, size-exclusion chromatography, and various preparative HPLC steps. The use of a range of 2D NMR measurements, in particular $^{13}C$-$^{13}C$ correlation measurements, has led to the clarification of the structure of kodaistatin A. Kodaistatin C is a hydroxylated derivative of kodaistatin A. Both natural products contain hydroxylated aspulvinones and identical highly substituted polyketide units. An X-ray single crystal structure analysis of aspulvinon E demonstrated the *z*-configuration at the central double bond. The kodaistatins are effective inhibitors of the glucose-6-phosphate translocase component of the glucose-6-phosphatase system (EC 3.1.3.9), an enzyme system which is important for the control of blood glucose levels. The $IC_{50}$ is 80 nM for kodaistatin A and 130 nM for kodaistatin C.

One characteristic of diabetes is the increased blood-glucose concentration. In the case of insulin-dependent or type I diabetes this is caused by the death of the insulin-producing $\beta$-cells of the pancreas, so treatment is by administration of insulin. By contrast, non-insulin-dependent or type II diabetes is characterized by reduced insulin activity in the muscle and fatty tissue (insulin resistance) and increased glucose production in the liver[1]. Active substances which can reduce the formation of glucose in the liver are therefore of particular interest in the treatment of type II diabetes.

The glucose released into the blood by the liver may be formed by the breakdown of glycogen stored in the liver (glycogenolysis) or by gluconeogenesis. Glucose-6-phosphate (G-6-P) is the common end-product of gluconeogenesis and glycogenolysis. The common step in the hepatic release of glucose from G-6-P is catalyzed by glucose-6-phosphatase (EC 3.1.3.9). Glucose-6-phosphatase is an enzyme complex made up of glucose-6-phosphate translocase (G-6-P-T1), glucose-6-phosphatase, and a phosphate translocase[2]. Of these components, G-6-P-T1 is highly selective, and is therefore a suitable target for the control of hepatic glucose release. Chlorogenic acid has been reported to be a weak inhibitor of G-6-P-T1[3]. The synthetic derivatives which have been described[4,5] inhibit glucose-6-phosphate translocase at concentrations in the nM or $\mu$M range.

Novel inhibitors of G-6-P-T1, called kodaistatins, have been found in cultures of the fungus *Aspergillus terreus* Thom DSM 11247[6]. In the present publication we report the isolation, characterization, and structural elucidation of these compounds which can inhibit glucose-6-phosphate

translocase specifically at submicromolar concentrations even in their native form.

## Experimental

### Analytical Detection of Kodaistatins (HPLC)

25 ml of culture solution of *Aspergillus terreus* Thom DSM 11247 was centrifuged and the clear supernatant (20 ml) or an extract of mycelium in 20 ml of 30% methanol was transferred onto 1 ml of 75~150 $\mu$m adsorption resin CHP20P (MCI GEL, Mitsubishi Chemical Corporation, Tokyo, Japan). The loaded resin was eluted with 4 ml of pure methanol. The kodaistatin content of the methanolic solution was determined by HPLC, without further processing. The stationary phase was either 250/4 Nucleosil 100-5 C18 HD (Macherey-Nagel, Düren, Germany) or LiChrospher RP-select B, 5 $\mu$m, 250×4 mm (E. Merck, Darmstadt, Germany). Column temperature: 40°C. Mobile phase: 45% acetonitrile in 0.1% orthophosphoric acid. At a flow rate of 1.0 ml/minute the retention time for kodaistatin A was 6.0 minutes. A Hewlett Packard Series 1100 instrument was used.

### Extraction and Purification of the Inhibitors

The culture solution (200 liters) from an *Aspergillus terreus* Thom DSM 11247 fermentation was clarified using a filter press. The kodaistatins were extracted from the aqueous phase by the addition of 5 kg of Amberlite XAD 7 to the culture filtrate (170 liters). The loaded resin was then eluted with 20 liters of methanol, and subsequent concentration under reduced pressure gave the crude kodaistatin extract. The mycelium (30 liters) was extracted with 2×50 liters of 30% aqueous methanol. The methanolic cell extract and water-diluted crude extract were loaded onto a CHP20P MCI GEL column (20 cm i. d.×50 cm, 15 liters) and separated using a gradient elution from 150 liters of 3 mM pH 7 sodium phosphate buffer to 150 liters of 2-propanol. The flow rate was 15 liters/hour and thirty 10-liter fractions were collected. Fraction 21 contained kodaistatin C, and fractions 22 and 23 contained the inhibitor kodaistatin A. Each of these fractions was concentrated under reduced pressure and freeze-dried. Further separation of fraction 21 and of fractions 22 and 23 was carried out on 4 liter Fractogel HW 40 columns (10 cm i. d.×50 cm high). The column was first eluted with 5 liters of pure water, followed by 40% acetonitrile in 10 mM of pH 7.0 potassium phosphate buffer. The flow rate was 33 ml/minute. After examination by HPLC the fractions eluted with acetonitrile were combined according to their kodaistatin A or C content and dried under reduced pressure. 90% pure material was obtained by preparative HPLC on LiChrosorb RP-select B (7 $\mu$m, 25 mm i. d.×250 mm high) using 25% acetonitrile in 10 mM pH 7 potassium phosphate buffer at a flow rate of 25 ml/minute. Desalting and final purification were carried out on the same solid phase under the same conditions, but using 30% acetonitrile in 0.1% trifluoroacetic acid as eluent. After freeze-drying this produced 120 mg of 98% pure kodaistatin A and the same procedure gave 11 mg of 96% pure kodaistatin C.

### NMR Measurements and Sample Preparation

NMR samples were prepared by dissolving 100 mg of kodaistatin A in 0.5 ml methanol-$d_4$ and 5 mg of the compound in DMSO-$d_6$. Wilmad NMR tubes (grade 528) with a diameter of 5 mm were used.

All spectra except NOESY measurements were recorded on a BRUKER DRX600 spectrometer operating at 600.13 MHz and 150.92 MHz for $^1$H and $^{13}$C respectively. The NOESY spectrum was acquired on a BRUKER DRX500 operating at 500.13 MHz ($^1$H) and 125.76 ($^{13}$C). The sample temperature was set at 278 K for the methanol-$d_4$ sample and 300 K for the sample in DMSO-$d_6$.

For the homonuclear experiments (double quantum filtered [DQF]-COSY[7,8], $^1$H-$^1$H NOESY[9,10]) the spectral width was set to 9 ppm in both dimensions, $F_1$ and $F_2$, and 8 transients were averaged for each $t_1$ value. In DQF-COSY experiments 1024 increments in $t_1$ were recorded with 2048 complex data points in $t_2$. NOESY spectra were recorded with 512 increments in $t_1$ and 2048 complex data points in $t_2$. Mixing times of 50, 100, 200, 300 and 500 ms were used.

To record the heteronuclear multiple quantum correlation (HMQC) spectra[11] 512 increments with 8 scans each and 2048 complex data points in $t_2$ were collected using sweep widths of 9 ppm in the proton dimension and 160 ppm in the carbon dimension. A bilinear rotation decoupling (BIRD) pulse was applied to suppress magnetization of protons bound to $^{12}$C. A delay of 3.45 ms, corresponding to 145 Hz, was used for the evolution of $^1$H-$^{13}$C one-bond couplings. The heteronuclear multiple bond correlation (HMBC) spectra[12] were acquired with a sweep width of 9 ppm in the proton dimension and 220 ppm in the carbon dimension. 1024 increments in $t_1$ and 2048 complex data points in $t_2$ were recorded. The delay for the evolution of long-range correlations was set to correspond to $^nJ_{CH}$ coupling constant values of 7 Hz. 8 scans per increment were collected.

Incredible natural abundance double quantum transfer experiments (INADEQUATE)[13] were recorded with delays

optimized for the evolution of $^{13}C$-$^{13}C$ one-bond couplings of 35, 50, and 70 Hz. Sweep widths of 210 ppm in $F_2$ and 420 ppm in $F_1$ (double quantum dimension) were used and 256 increments in $t_1$ with 2048 complex data points in $t_2$ were recorded. A total of 2048 transients were averaged per $t_1$ increment.

Before Fourier transformation all time domain data were subjected to apodization using adjusted exponential, sine and squared sine bell window functions. The software packages XWINNMR and AURELIA supplied by Bruker, Rheinstetten, Germany, were used for data processing.

X-Ray Single-crystal Structural Analysis of Aspulvinone E

Crystals were obtained by recrystallization from methanol. A crystal of dimensions 0.2* 0.07* 0.01 $mm^3$ was sealed in a Lindemann glass capillary. All the measured reflections were used to determine the cell parameters (a=28.987(2), b=12.815(1), c=7.051(1) Å, $\alpha$=90.0(1), $\beta$=90.5(1), $\gamma$=90.0(1)°, Z=8, P-1) on a computer-controlled four-circle diffractometer equipped with a CCD area detector (SIEMENS) and a low-temperature device (−80°C). The intensities were measured on the same apparatus ($\omega$- and $\varphi$-scans with a step width of 0.3°, measuring time 120 s/frame): Mo-K$\alpha$ radiation (X-ray generator with a rotating anode: 0.5×5 $mm^2$ focus, 50 kV, 140 mA), 6638 reflections ($\vartheta_{min}$=2.11, $\vartheta_{max}$=19.78; −27<h<27, −12<k<12, −6<l<4, resolution: 1.05 Å), 3682 of which were unique ($R_{int}$=0.1545, $R_\sigma$=0.1781), and they were all used for the structural analysis. Direct methods were used to solve the phase problem[14], only an isotropic refinement of the thermal parameters by least-squares methods made sense[15] {minimization of $(F_o^2-F_c^2)^2$; weighting scheme: $w=1/[\sigma^2(F_o^2)+(0.0292*P)^2+139.26*P]$, $P=[Max(F_o^2,0)+2*Fc^2]/3$, where $\sigma$ is based on the counting statistics, 354 parameters, 348 restraints}, the coordinates of the H atoms were calculated on the basis of the geometrical requirements, S=1.125, R=0.1861 for $|F_o|>4\sigma$, 2053 reflections, $R_w$=0.4342, minimum and maximum peak in the difference map: −0.572 and 0.670 electrons/Å$^3$. The data and the results were not significant enough to confirm the monoclinic space group $P2_1/c$. The structure analysis was done in the triclinic space group P1- and with 4 molecules in the asymmetric unit. All calculations were done by a DEC 3000/900 AXP with the SHELXS-90[14], SHELXTL-PLUS[16] and SHELXL-97[15] programs.

The average estimated standard deviation (e.s.d.) of a C–C bond is 0.016 Å and that one of an O–C bond 0.014 Å. The average e.s.d. of C–C–C bond angles is 1.30° and that one of C–C–C–C torsion angles 4.0°.

Microsomal Glucose-6-phosphatase Activity Assay

Hepatic microsomes were prepared as described previously and stored frozen at −70°C at a protein concentration of 15~20 mg per ml[17]. The intactness of the preparations, quantified from the latency of mannose-6-phosphatase activity[18], was usually above 97%. Detergent-disrupted microsomes were prepared according to published procedures[17] by exposing thawed microsomes (2 mg protein/ml) to 0.1% Triton X-100™ for 20 minutes at 4°C. Under these conditions it is possible to produce maximum release of latent activity while leaving the glucose-6-phosphatase catalytic unit unaffected. We evaluated the specific inhibitory potency of kodaistatins on glucose-6-phosphate translocase by assessing their effect on phosphohydrolase activity of "untreated" and detergent-disrupted microsomes. (The term "untreated" is used to designate microsomal vesicles that are prepared and used without further treatment.) In untreated microsomes from fasted rats, T1 translocase imposes significant rate limitations on the steady-state hydrolysis of glucose-6-phosphate, whereas other translocase components play no significant role under these conditions. The hydrolysis of inorganic pyrophosphate by untreated microsomes provided an assay for T2, the phosphate translocase[19]. Hydrolysis of glucose-6-phosphate, mannose-6-phosphate and sodium pyrophosphate was assayed in the presence or absence of test compound (0.01~100 $\mu$M) by quantification of inorganic phosphate in a previously described colorimetric assay scaled down to accommodate assay volumes of 300 $\mu$l. Stock solutions of test compounds in DMSO were diluted with assay buffer. The resulting maximal DMSO concentration of 1% (v/v) had no effect on the intactness of microsomes or on phosphatase activity (results not shown). The $IC_{50}$ values of test compounds were routinely determined by non-linear least-squares analysis of the inhibition values obtained from at least 2 independently performed experiments with a difference in inhibition values between experiments of less than 10%.

## Results and Discussion

The kodaistatin content of the culture solutions and the presence or absence of kodaistatins in the cell mass or culture filtrate are extremely fermentation-dependent. An enrichment procedure with subsequent isocratic HPLC was therefore used to assess the microbiological yields. Since cultures of *Aspergillus terreus* Thom DSM 11247 contain a great variety of metabolic products, only substances showing ultraviolet absorption at 368 nm were recorded, the

Table 1. Physico-chemical properties of kodaistatins A and C.

| | Kodaistatin A | Kodaistatin C |
|---|---|---|
| Appearance | Yellow solid | Yellow solid |
| $[\alpha]_D^{21}$ | -86° (c 0.04, MeOH) | -20° (c 0.04, MeOH) |
| Molecular formula | $C_{35}H_{34}O_{11}$ | $C_{35}H_{34}O_{12}$ |
| HR FAB-MS (*m/z*) | 631.2174 $(M+H)^+$ | 647.2141 $(M+H)^+$ |
| Calculated | 631.2179 | 647.2129 |
| UV $\lambda_{max}^{MeOH}$ nm (log ε) | 292 (4.66), 333 (Sh) | 288, 333 (Sh) |
| $\lambda_{max}^{MeOH+0.1N\ HCl}$ nm (log ε) | 238 (4.35), 294 (4.51), 368 (4.30) | 242 (Sh), 292, 378 |
| Solubility | | |
| Soluble in | Acetonitrile, MeOH, DMSO | MeOH, DMSO |
| HPLC retention time | 12.3 minutes[a] | 8.65 minutes[a] |

[a]Column: 250/4 Nucleosil 100-5 C18 HD (Macherey-Nagel, Düren, Germany). Eluent: 45% acetonitrile in 0.1% trifluoroacetic acid, flow rate 1.0 ml/minute.

kodaistatins among them being identified from their UV spectra recorded using a diode-array detector.

To isolate the kodaistatins, 3% Amberlite XAD 7 adsorption resin was added to the *Aspergillus terreus* Thom DSM 11247 culture filtrate, then the kodaistatin was washed out of the adsorption resin by elution with methanol. If kodaistatins were present in the mycelium, the cell mass was extracted with 30% aqueous methanol. The alcohol concentration was chosen so as to dissolve the desired inhibitors while leaving non-polar impurities such as lipids undiluted.

The concentrates from the XAD eluate and the cell extract were then chromatographed on MCI GEL adsorption resin, acting as a reversed-phase solid phase, using a gradient procedure with 2-propanol. Alternatively, the kodaistatin from the crude extract can be enriched using an anion exchanger: the slightly acidic kodaistatins are loaded onto the DEAE ion exchanger under neutral conditions and, to avoid salt contamination, eluted with 0.2% trifluoroacetic acid in 50% acetonitrile (buffer B). The concentrated, enriched inhibitor-containing fractions from the preliminary purification were further separated by size-exclusion chromatography. Water was used as the first solvent, to remove polar impurities, and was followed by 40% acetonitrile in 10 mM, pH 7, phosphate buffer to separate off lipophilic compounds. Final purification of the kodaistatins was carried out by preparative reversed-phase chromatography, first in a phosphate buffer/acetonitrile system, followed by a second chromatographic step with 0.1% trifluoroacetic acid/acetonitrile as the mobile phase to remove the salts. The freeze-dried kodaistatin A thus obtained was >98% pure. The strain *Aspergillus terreus* Thom DSM 11247 produces kodaistatin A as the main component, with smaller quantities of kodaistatin C. The components B and D, which occur only in traces, are isomers of compounds A and C respectively. Fig. 2 illustrates the purification procedure schematically, and Table 1 shows the physicochemical data for the main components. As an *ortho*-diphenol, kodaistatin A is gradually oxidized in air, and the more sensitive di-*ortho*-diphenol kodaistatin C is stable only in the absence of oxygen. All investigations were carried out with freshly prepared material.

## Mass-Spectral Data

Elemental analysis showed that kodaistatin A consists only of carbon, hydrogen and oxygen. High-resolution fast atom bombardment (FAB) mass spectrometry (MS) yielded $m/z$=631.2174 $(M+H)^+$. The high-resolution mass agreed most closely with the chemical formula $C_{35}H_{34}O_{11}$ (devia-

Fig. 1. Chemical structures of kodaistatins A and C.

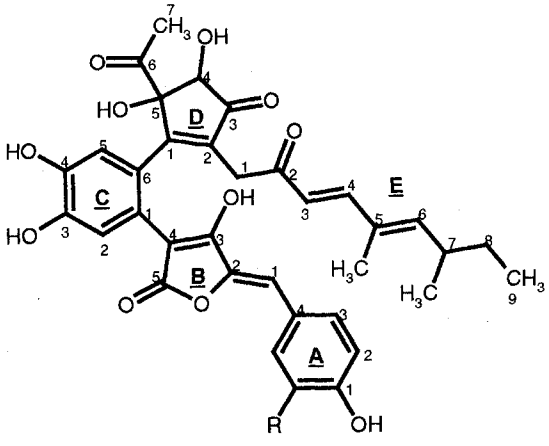

Kodaistatin A : R = H
Kodaistatin C : R = OH

tion: 0.5 milli-atomic mass units).

NMR Structural Analysis

The structure of kodaistatin A (Fig. 1) was determined by a wide range of NMR investigations. Assignment of the proton and carbon resonances in methanol-$d_4$ and DMSO-$d_6$ (Table 2) was achieved using various NMR techniques including DQF-COSY, NOESY, HMQC, HMBC and INADEQUATE spectra.

In Fig. 3 the $^{1}H$-$^{13}C$ long-range correlations in the HMBC spectrum are depicted by arrows. The chemical structure of side chain E was unambiguously defined by the correlations shown. In addition, this substructure was confirmed by the homonuclear couplings observed in the DQF-COSY spectrum (spin system E9 to E5-Methyl and E3, E4). A homonuclear coupling constant of 16 Hz between protons E3 and E4 prove that the double bond is *E* configurated. Strong NOE correlations between protons E4/E6 and E5-Methyl/E7-Methyl and a weak NOE effect between E5-Methyl and E6 supported the same configuration (*E*) for double bond E5/E6. All $^{13}C$-$^{13}C$ one-bond correlations for side chain E except the one between E1 and E2 were observed in the INADEQUATE spectrum (Fig. 4).

Unambiguous identification and resonance assignment were also achieved for the para-hydroxyphenyl moiety A on the basis of the observed correlations in the HMBC, DQF-COSY and INADEQUATE spectra.

Owing to the low number of protons in rings B and D, only a limited number of $^{1}H$-$^{13}C$ long-range correlations were detected in the HMBC spectrum, leaving some ambiguities for these substructures. These were resolved by correlations in the INADEQUATE spectrum. In ring D the connection of carbons D2 to D5 was established by $^{13}C$-$^{13}C$ one-bond correlations, as was the bond between D2 and E1. The position of D1 was determined by a strong ($^{3}J_{CH}$) correlation between $C_{D1}$ and $H_{E1}$ and a weak ($^{4}J_{CH}$) correlation between $C_{D5}$ and $H_{E1}$ in the HMBC spectrum. In addition, the observed chemical shifts for ring D are in accordance with the structure of this fragment. The linkage of the substructures D and E was proved by heteronuclear couplings between proton E1 and carbons D1, D2, D3 and D5, as well as by the above mentioned one-bond correlation of carbon D2 and E1.

For ring B the connection of the stretch B1 to B3 could be followed in the INADEQUATE spectrum. The one-bond correlations between B3, B4 and B5 seemed too weak to be detected by the experiment. However, the observed heteronuclear couplings in the HMBC spectrum and the carbon chemical shifts are in accordance with the same $\gamma$-lactone structure seen in aspulvinone E. Fragments A and B are linked by correlations in the INADEQUATE ($C_{A4}/C_{B1}$) and HMBC ($C_{A4}/H_{B1}$, $C_{A3}/H_{B1}$, $C_{B1}/H_{A3}$, $C_{B2}/H_{A3}$) spectra.

Despite the large number of $^{1}H$-$^{13}C$ long-range correlations observed for ring C, it was impossible on the basis of the HMBC data alone to distinguish between the shown *o*-hydroquinone and a *p*-hydroquinone structure in which the substituent positions of the hydroxyl function and ring B are interchanged. Both structures were in accordance with the correlations detected. The identification of ring C as an *o*-hydroquinone was straightforward on the basis of the observed $^{13}C$-$^{13}C$ one-bond correlations in the INADEQUATE spectra (see Fig. 4), which firmly ruled out the *p*-hydroquinone alternative. The connection of rings B and D to positions C1 and C6 of the *o*-hydroquinone was demonstrated both by the carbon one-bond correlations in the INADEQUATE spectrum and by the heteronuclear

Aspulvinon E

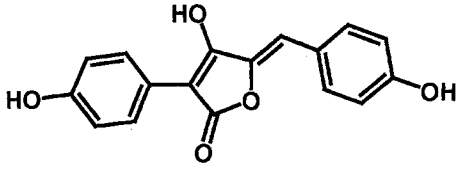

Table 2. $^{1}H$ and $^{13}C$ NMR data for kodaistatin A in methanol-$d_4$ at 278 K and in DMSO-$d_6$ at 300 K.

| Position | Methanol-$d_4$ | | DMSO-$d_6$ | |
|---|---|---|---|---|
| | $^{1}H$ | $^{13}C$ | $^{1}H$ | $^{13}C$ |
| A1 | - | 160.14 | - | 158.45 |
| A2 | 6.84 d | 116.89 | 6.83 d | 115.77 |
| A3 | 7.62 d | 133.92 | 7.55 d | 131.97 |
| A4 | - | 125.45 | - | 123.70 |
| B1 | 6.20 s | 110.71 | 6.23 s | 107.58 |
| B2 | - | 142.01 | - | 140.71 |
| B3 | - | 166.51 | - | 165.00 |
| B4 | - | 102.86 | - | 100.82 |
| B5 | - | 172.74 | - | 170.30 |
| C1 | - | 121.65 | - | 120.00 |
| C2 | 6.87 s | 118.77 | 6.77 s | 117.76 |
| C3 | - | 147.93 | - | 146.21 |
| C4 | - | 146.95 | - | 145.38 |
| C5 | 6.40 s | 114.76 | 6.29 s | 113.46 |
| C6 | - | 124.24 | - | 122.65 |
| D1 | - | 163.69 | - | 161.61 |
| D2 | - | 139.12 | - | 137.24 |
| D3 | - | 202.65 | - | 200.01 |
| D4 | 4.54 s | 86.32 | 4.26 s | 84.45 |
| D5 | - | 91.69 | - | 89.66 |
| D6 | - | 210.05 br | - | 207.71 |
| D7 | 2.46 s | 28.52 br | 2.32 s | 27.69 |
| E1 | 3.48 d/3.23 d | 38.69 | 3.29 d/3.06 d | 36.91 |
| E2 | - | 196.65 | - | 194.09 |
| E3 | 6.02 d | 122.94 | 5.93 d | 122.60 |
| E4 | 6.96 d | 149.93 | 6.92 d | 147.21 |
| E5 | - | 133.37 | - | 131.62 |
| E5-Me | 1.75 s | 12.76 | 1.70 s | 12.11 |
| E6 | 5.48 d | 151.51 | 5.57 d | 148.67 |
| E7 | 2.46 m | 36.31 | 2.44 m | 34.22 |
| E7-Me | 1.02 d | 20.85 | 0.97 d | 19.94 |
| E8 | 1.34 m/1.22 m | 31.13 | 1.34 m/1.21 m | 29.35 |
| E9 | 0.80 t | 12.51 | 0.78 t | 11.63 |

couplings in the HMBC spectrum.

Along with kodaistatins, the known secondary metabolites flavipine[20], flavipucine[21] and aspulvinone E[22] were isolated from cultures of *Aspergillus terreus* Thom DSM 11247. Aspulvinones[23] are members of a group of closely-related natural products, the substituted 4-hydroxy-3-(4-hydroxyphenyl)-5-[(4-hydroxyphenyl)-methylene]-2(5*H*)-furanones.

To confirm the configuration of the exocyclic double bond, the structure of aspulvinone E[22], the parent compound of this series, was investigated by X-ray structural analysis (Fig. 5) and the NMR data were compared with those of kodaistatin A.

In terms of the benzylidene double bond, the benzylidene and the oxygen of the 5-membered ring have the *Z*-configuration. This had previously been tacitly assumed to be the case for aspulvinone E, but to our knowledge it had not previously been demonstrated. The benzylidene and phenyl rings are positioned at angles of 15.7(9) and 24.4(9), 3.5(13) and 22.2(10), 14.9(9) and 25.5(9) and 4.4(12) and

Fig. 2. Isolation procedure for kodaistatins A and C.

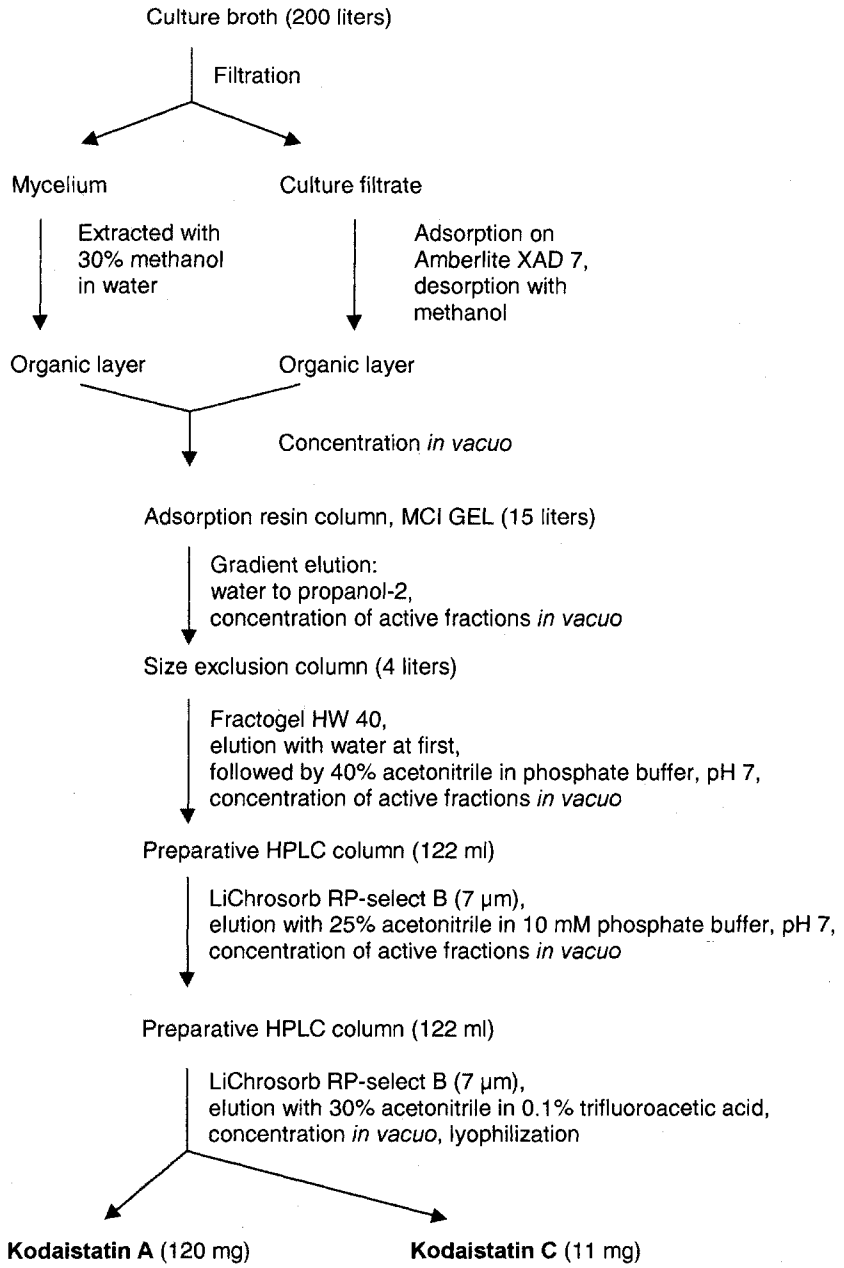


22.3(10)° relatively to the central 5-membered rings in the four molecules of the asymmetric unit. The small size of the used crystal ($0.2\times0.07\times0.01\,mm^3$) and the resultant extremely weak reflections necessitated at the end calculations in the space group P 1- (as already mentioned), although the dihedral angles cited above are almost consistent with the monoclinic space group $P2_1/c$. Interesting are the differences of the hydrogen bond lengths O–H...OH (2.74 (2) to 2.85 (3) Å) and–OH...O=C (2.57 (2) to 2.60 (2) Å). The average values are 2.79 and 2.58 Å respectively.

The fact that the measured NMR signals of aspulvinone E correspond to the NMR data for rings A, B, and C of kodaistatin provides additional confirmation of the substructure and configuration of the new inhibitor in the region of the aromatic rings.

Accordingly, the structure of the kodaistatins includes two characteristic units: one half is made up of the aromatic substituted aspulvinone and the other the highly substituted ring D. The latter has structural similarities to the

azaphilone[24]-type polyketides which are often found in fungal cultures.

The structural analysis does not clarify the stereochemical arrangement of the OH groups on ring D. Initial attempts at derivatization did not produce products which would permit assignment of the configuration.

## Biological Activities

Reduction of the inappropriate hepatic glucose production that is commonly observed in type II diabetes[25]

Fig. 4. Result of the INADEQUATE experiments of kodaistatin A.

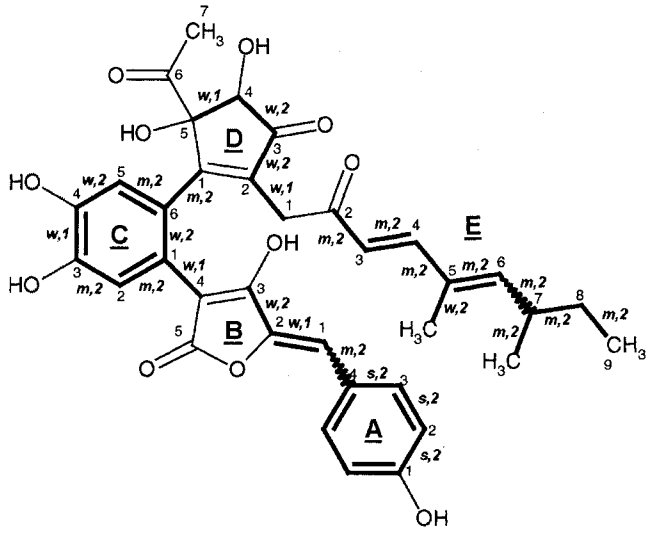

Three spectra were recorded, optimized to $^{1}J_{CC}$ coupling constants of 35, 50 and 70 Hz. The spectra were added for analysis. Observed C–C connections are indicated by bold bonds. Signal intensities are shown as w (weak), m (medium) and s (strong). The observation of both signals or only one signal at a corresponding double quantum frequency is indicated by 2 or 1 respectively.

Fig. 3. $^{1}H$-$^{13}C$ long-range correlations observed in the HMBC spectrum of kodaistatin A.

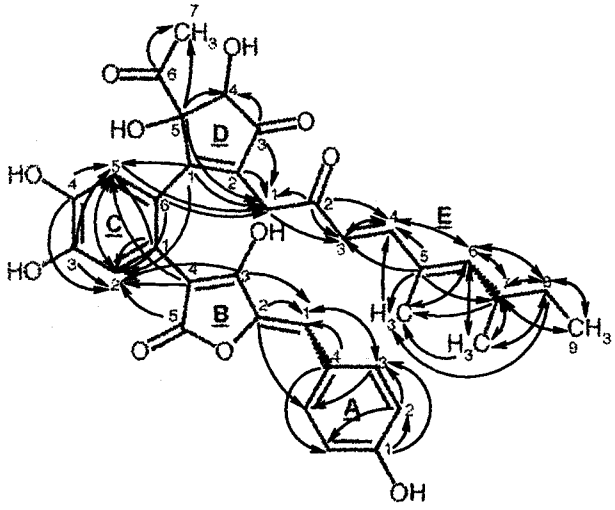

Arrows originating at the carbon atoms and pointing toward the correlated protons mark the correlations detected. For reasons of clarity the chemical formula is shown by shaded lines.

Fig. 5. The four independent molecules of aspulvinone E in the asymmetric unit, showing the atom numbering and thermal spheres (30% probability level)

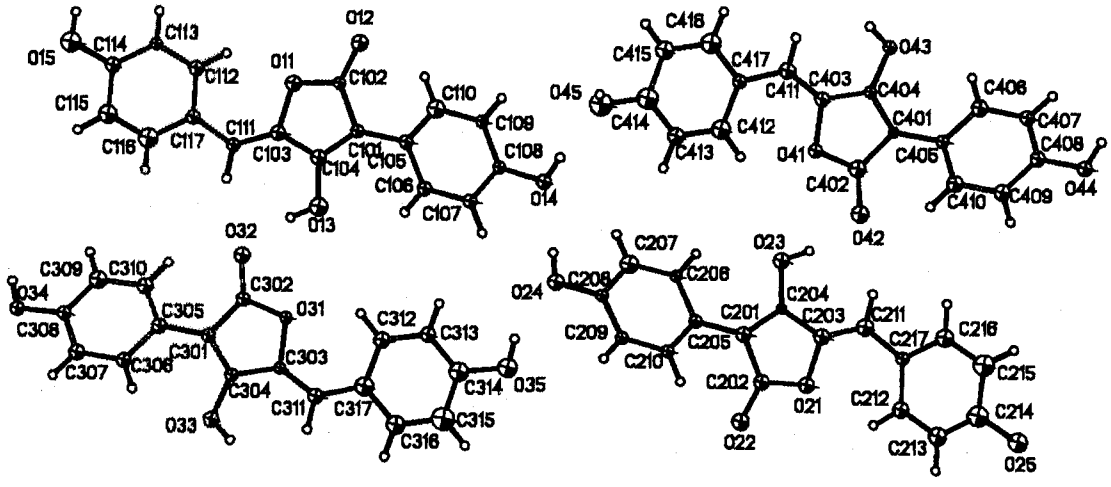

is a promising target for therapeutic intervention in type II diabetes. Glucose produced by the liver can be derived either from gluconeogenesis or glycogenolysis. The enzyme system glucose-6-phosphatase (gl-6-Pase, E.C. 3.1.3.9) is localized in the membranes of the endoplasmic reticulum and catalyzes the terminal step of both glucose-producing pathways. Inhibition of glucose-6-phosphatase activity can be expected to reduce hepatic glucose production arising from both of these glucose-producing pathways.

In the present study, we identified kodaistatins as potent inhibitors of the glucose-6-phosphate translocase component of the glucose-6-phosphatase system of the rat liver endoplasmic reticulum. The compounds specifically inhibit the glucose-6-phosphate translocase that is responsible for the transport of glucose-6-phosphate from the cytosol into the lumen of the endoplasmic reticulum.

Kodaistatin A inhibited glucose-6-phosphatase activity in untreated rat liver microsomes with an $IC_{50}$ of 0.08 $\mu$M. In contrast, the pyrophosphatase activity of untreated microsomes remained unaffected, and disruption of the microsomal membranes completely abolished the inhibition of glucose-6-phosphatase activity observed in untreated microsomes. Kodaistatin C inhibited glucose-6-phosphatase activity in untreated rat liver microsomes with an $IC_{50}$ of 0.13 $\mu$M, and, like kodaistatin A, showed no effect on the glucose-6-phosphatase activity in disrupted microsomes. These results suggest that kodaistatins A and C specifically interact with T1, the glucose-6-phosphate translocase of the glucose-6-phosphatase system[26], although definite proof of the specificity of kodaistatin C for Gl-6-P translocase would require the exclusion of an effect of the compound on the pyrophosphatase activity in untreated microsomes, as has been demonstrated for kodaistatin A.

Aspulvinone E only slightly inhibited the glucose-6-phosphatase activity of untreated microsomes. Its $IC_{50}$ is 200 $\mu$M, representing 2500-times weaker inhibition than that of kodaistatin A. The aromatic dialdehyde flavipine is more effective, with an $IC_{50}$ of about 15 $\mu$M.

## References


1) ASHMORE, J. & G. WEBER: The role of hepatic glucose-6-phosphatase in the regulation of carbohydrate metabolism. Vitamins Hormones 17: 91~132, 1959
2) BURCHELL, A. & I. D. WADDELL: The molecular basis of the hepatic microsomal glucose-6-phosphatase system. Biochim. Biophys. Acta 1092: 129~137, 1990
3) SCHINDLER, P. W.; P. BELOW, H. HEMMERLE, H.-J. BURGER, K. H. S. SWAMY, W. J. ARION, S. EFENDIC & A. W. HERLING: Identification of two new inhibitors of the hepatic glucose-6-phosphatase system. Drug Development Research 44: 34~40, 1998
4) HEMMERLE, H.; H.-J. BURGER, P. BELOW, G. SCHUBERT, R. RIPPEL, P. W. SCHINDLER, E. PAULUS & A. W. HERLING: Chlorogenic acid and synthetic chlorogenic acid derivatives: novel inhibitors of hepatic glucose-6-phosphate translocase. J. Medicinal Chem. 40: 137~145, 1997
5) KRAMER, W.; H.-J. BURGER, W. J. ARION, D. CORSIERO, F. GIRBIG, C. WEYLAND, H. HEMMERLE, S. PETRY, P. HABERMANN & A. W. HERLING: Identification of protein components of the microsomal glucose 6-phosphate transporter by photoaffinity labeling. Biochem. J. 339 (Pt 3): 629~638, 1999
6) RAMAKRISHNA, N. V. S.; K. H. S. SWAMY, K. JAYVANTI, S. R. NADKARNI, E. K. S. VIJAYAKUMAR, A. HERLING, H. KOGLER & L. VÉRTESY: Kodaistatins, novel Inhibitors of Glucose-6-phosphate Translocase T1 from *Aspergillus terreus* Thom DSM 11247. International publication number: WO 98/47888
7) PIANTINI, U.; O. W. SORENSEN & R. R. ERNST: Multiple quantum filters for elucidating NMR coupling networks. J. Am. Chem. Soc. 104: 6800, 1982
8) RANCE, M.; O. W., SORENSEN, G., BODENHAUSEN G., WAGNER R. R. ERNST & K. WÜTHRICH: Improved spectral resolution in COSY proton NMR spectra of proteins via double quantum filtering. Biochem. Biophys. Res. Commun. 117: 479~485, 1983
9) JEENER, J.; B. H. MEIER, P. BACHMANN & R.R. ERNST: Investigation of exchange processes by two-dimensional NMR spectroscopy. J. Chem. Phys. 71: 4546~4553, 1979
10) KUMAR, A.; R.R. ERNST & K. WUETHRICH: A two-dimensional nuclear Overhauser enhancement (2D NOE) experiment for the elucidation of complete proton-proton cross-relaxation networks in biological macromolecules. Biochem. Biophys. Res. Commun. 95: 1~6, 1980
11) BAX, A. & S. SUBRAMANIAN: Sensitivity-enhanced two-dimensional heteronuclear shift correlation NMR spectroscopy. J. Magn. Reson. 67: 565~569, 1986
12) BAX, A. & M. F. SUMMERS: $^{1}H$ and $^{13}C$ Assignments from sensitivity-enhanced detection of heteronuclear multiple-bond connectivity by two-dimensional multiple quantum NMR. J. Am. Chem. Soc. 108: 2093~2094, 1986
13) BAX, A.; R. FREEMAN & T. A. FRENKIEL: An NMR technique for tracing out the carbon skeleton of an organic molecule. J. Am. Chem. Soc. 103(8): 2102~2104, 1981
14) SHELDRICK, G. M.: SHELXS-90. Program for the Solution of Crystal Structures. University of Göttingen, 1990
15) SHELDRICK, G. M.: SHELXL-97. Program for the Refinement of Crystal Structures. University of Güttingen, Germany, 1993
16) SHELDRICK, G. M.: SHELXTL-PLUS, Release 4.1, An Integrated System for Solving, Refining and Displaying Crystal Structures from Diffraction Data. Siemens Analytical x-ray Instruments Inc., Madison, Wisconsin, USA, 1991
17) ARION, W. J.; W. K. CANFIELD, F. C. RAMOS, M. L. SU, H.-J. BURGER, H. HEMMERLE, G. SCHUBERT, P. BELOW & A. W. HERLING: Chlorogenic acid analogue S 3483: a potent competitive inhibitor of the hepatic and renal glucose-6-phosphatase systems. Arch. Biochem.

Biophys. 351: 279~285, 1998

18) ARION, W. J.: Measurement of intactness of rat liver endoplasmatic reticulum. Methods of Enzymology. Volume 174: 58~67, Academic Press, Inc. 1989

19) ARION, W. J.; A. J. LANGE, H. E. WALLS & L. M. BALLAS: Evidence for the participation of independent translocases for phosphate and glucose-6-phosphate in the microsomal glucose-6-phosphate system. J. Biol. Chem. 255: 10396~10406, 1980

20) RAISTRICK, H. & P. RUDMAN: Biochemistry of microorganisms- XCVII. Flavipine, a crystalline metabolite of *Aspergillus flavipes* and *Aspergillus terreus*. Biochem. J. 63: 395~407, 1956

21) SASSA, T. & Y. ONUMA: Isolation and identification of fruit rot toxins from the fungus-caused *Macrophoma* fruit rot of apple. Agric. Biol. Chem. 47: 1155~1157, 1983

22) SUGIYAMA, H.; N. OJIMA, M. KOBAYASHI, Y. SENDA, J. ISHIYAMA & S. SETO: Carbon-13 NMR spectra of aspulvinones. Agric. Biol. Chem. 43: 403~404, 1979

23) BERGLEY, M. J.; D. R. GEDGE, D. W. KNIGHT & G. PATTENDEN: Aspulvinones, a new class of natural products from *Aspergillus terreus*. Re-investigation of structures by x-ray crystallographic and spectrometric analysis. J. Chem. Soc. Perkin I, (1979) Issue 1: 77~83, 1979

24) MATSUZAKI, K.; H. TAHARA, J. INOKOSHI & H. TANAKA: New brominated and halogen-less derivatives and structure-activity relationship of azaphilones inhibiting gp120-CD4 binding. J. Antibiotics 51: 1004~1011, 1998

25) DEFRONZO, R. A.; E. FERRANNINI & D. C. SIMONSON: Fasting hyperglycemia in non-insulin-dependent diabetes mellitus: contributions of excessive hepatic glucose production and impaired tissue glucose uptake. Metabolism. 38: 387~395, 1989

26) BURGER, H.-J.; W. J. ARION, K. H. S. SWAMY, M. KNAUF, L. VÉRTESY & A. W. HERLING: Kodaistatin A, a new inhibitor from *Aspergillus terreus* of the hepatic glucose-6-phosphatase system. Abstracts of the Annual Meeting of the American Diabetes Association. June 19~22, 1999, San Diego, USA